Available online at www.sciencedirect.com
ScienceDirect

Thermochimica Acta 465 (2007) 30–39

thermochimica acta

www.elsevier.com/locate/tca

Determination of the adsorption heat of *n*-hexane and *n*-heptane on zeolites beta, L, 5A, 13X, Y and ZSM-5 by means of quasi-equilibrated temperature-programmed desorption and adsorption (QE-TPDA)

Wacław Makowski*, Łukasz Ogorzałek

Faculty of Chemistry, Jagiellonian University, Ingardena 3, 30-060 Krakow, Poland

Received 29 April 2007; received in revised form 31 August 2007; accepted 6 September 2007
Available online 14 September 2007

Abstract

Measurements of temperature-programmed desorption and adsorption of *n*-hexane and *n*-heptane under quasi-equilibrium conditions (QE-TPDA) were performed for several zeolites in TPD apparatus equipped with a TCD detector. One-step adsorption profiles for zeolites X and Y and two-step adsorption profiles for beta, L, 5A and ZSM-5 were observed. Approximate adsorption isobars calculated from the QE-TPDA profiles did not depend on the heating/cooling rate, proving equilibrium control of the adsorption degree. Values of the adsorption enthalpy and entropy, computed by fitting the Langmuir or dual site Langmuir model functions to the temperature derivatives of the experimental adsorption isotherms, were in agreement with the literature data. New method for determination of the initial (zero coverage) adsorption heat by fitting the linearized Henry function to the transformed high temperature experimental data was proposed. Values of the initial adsorption heat were close to those obtained using the inverse gas chromatography infinite dilution method.

Keywords: Adsorption; Temperature-programmed desorption; Initial adsorption heat; Zeolites; *n*-Hexane; *n*-Heptane

1. Introduction

Adsorption heat is a key parameter characterizing an adsorbate/adsorbent system. For adsorbents operating under isobaric conditions the isosteric adsorption heat, calculated from the adsorption isosters (either measured directly or constructed from the adsorption isotherms) is most often used [1].

The classical experimental methods for adsorption studies are based on volumetric or gravimetric measurements of the adsorption degree for a given partial pressure of the adsorptive. Such measurements are usually tedious and time consuming, they also require complicated and expensive instrumentation [2]. A faster but less accurate alternative of these methods is the inverse gas chromatography (IGC) [3]. Although IGC is a non-equilibrium method, usually it is assumed that elution of the adsorbate through the adsorbent bed proceeds via succession of quasi-equilibrium steps. Thus, basing on IGC chromatograms one may determine equilibrium characteristics of adsorption, such as the initial (zero-coverage) adsorption heat (in the infinite dilution range) [4] or the adsorption isotherms (in the finite dilution range) [4].

Quasi-equilibrium temperature-programmed desorption and adsorption (QE-TPDA) is new experimental technique also assuming equilibrium control of desorption degree. It was recently applied in studies of adsorption of *n*-hexane and *n*-heptane on ZSM-5, X and Y zeolites [5,6]. It has been shown that the desorption and adsorption profiles, measured in a standard temperature-programmed desorption setup with a TCD detector using carrier gas containing small admixture of the adsorptive, could be accurately fitted with a quasi-equilibrium models based on Langmuir or dual site Langmuir functions, despite changes of temperature and concentration of the adsorptive [6]. The equilibrium control of sorption has also been confirmed by linearity of the isosters constructed from the QE-TPDA profiles [6]. Values of the adsorption enthalpy and entropy, either determined from the adsorption isosters or as the fitted model parameters, were close to the literature data. However, the isosteric method of interpretation of the QE-TPDA profiles is not suited for routine

---

* Corresponding author. Tel.: +48 12 6632245; fax: +48 12 6340515.
E-mail address: makowski@chemia.uj.edu.pl (W. Makowski).

0040-6031/$ – see front matter © 2007 Elsevier B.V. All rights reserved.
doi:10.1016/j.tca.2007.09.002

measurements because of relatively long time of the measurements. It also requires high quality experimental data, free from diffusion limitations or major disturbances of the detector signal, otherwise uncertainty of the adsorption enthalpy and entropy is too large. Therefore this work was aimed at further development of the QE-TPDA method, especially on shortening of the measurements and simplifying the mathematical treatment of the experimental data, in order to make it more suitable as a screening technique allowing fast determination of the adsorption enthalpy, entropy and saturation sorption capacity. For verification of the results obtained from the QE-TPDA measurements another experimental technique, i.e. infinite dilution IGC was employed.

Another aim of this work was application of the equilibrated thermodesorption of *n*-hexane and *n*-heptane for characterizing the micropore structure of zeolites beta, L and 5A, in comparison to well studied zeolites X, Y and ZSM-5 [6–11]. Although the latter zeolites posses 3D systems of the micropores, they exhibit different profiles of *n*-alkane thermodesorption. For the FAU-type zeolites (X and Y) one-step desorption profiles are characteristic, corresponding to the type I adsorption isotherm. Complex two-step desorption profiles, observed for *n*-hexane and *n*-heptane on ZSM-5 zeolites, reveal a kind of order–disorder transition in the adsorbed phase, referred to as “commensurate freezing” [12]. Similarly, two-step TPD profiles reported for zeolites 5A [13] (possessing 3D regular LTA framework with large α-cages interconnected via 8 member-ring windows) were also attributed to entropy effects, related to loss of translational mobility at higher loadings. The micropore structure of zeolite beta (BEA), consisting of intersecting straight and sinusoidal (or zigzag) channels, is similar to that of ZSM-5 (MFI) [14], though the channel diameters in the BEA structure, corresponding to 12 MR windows, are slightly larger. For such a structure complex two-step thermodesorption profiles may also be expected. However, no equilibrated thermodesorption results have been yet published for zeolites beta, only simple adsorption isotherms of *n*-hexane with no inflection point, indicating one-step desorption pattern, were reported [14]. Similar simple isotherms may also be expected basing on limited adsorption data available for *n*-hexane on zeolites L [15], possessing 1D system of micropores formed by 12 MR windows.

2. Experimental

Commercial zeolites beta (H-BEA, Zeolyst, Si/Al = 180), L (K-LTL, Si/Al = 2.7, Union Carbide), 5A (CaNa-LTA, Si/Al = 1.0, Alltech, GC packing), 13X (Na-FAU, Si/Al = 1.25, Supelco, GC packing), Y (dealuminated H-FAU, Si/Al = 17 or >100, Degussa) and ZSM-5 (H-MFI, Akzo Nobel, Si/Al = 66) were used in this study. Analytical pure *n*-hexane and *n*-heptane (POCh, Poland) were used as sorbates. Apart from the preformed 13X (80/100 mesh) and 5A (60/80 mesh) all the other zeolites were pressed into pellets, crushed and sieved.

The QE-TPDA experiments were performed using a home-made temperature-programmed desorption setup that was described in detail earlier [5,6]. The setup was equipped with a thermal conductivity detector (Valco MicroVolume TCD) connected to the quartz tube (o.d. 6 mm, 15 cm long) containing the sample (ca 10 mg, 0.35–0.50 mm particles). Helium (5.0, Messer) was used as a carrier gas. The carrier gas line was equipped with a diffuser (a glass bulb containing the liquid hydrocarbon (HC) with the attached capillary) that was continuously adding a small admixture of the HC vapor to the stream of He. Using the diffuser stable concentrations of *n*-alkane in He of about 0.5 vol.% could be obtained even for prolonged periods. All the lines were heated in order to avoid any condensation or adsorption of the HC vapors.

Prior the QE-TPDA experiments each sample was activated by heating in a flow of pure He to 500 °C at 10 °C/min and then cooled down. After activation adsorption was performed at room temperature, by switching the flow of He/HC mixture through the reactor until a breakthrough in the TCD signal at the reactor outlet was observed. When the signal stabilized the QE-TPDA experiment was performed by heating the sample with the preadsorbed HC in the flow of He/HC mixture (7.5 cm^3/min) according to a temperature program consisting of several heating and cooling cycles (with the temperature change rates of 6, 4 and/or 2 °C/min), intervening with 30 min isothermal room temperature periods.

For the IGC measurements the zeolite sample (ca 1 g, the sieve fraction 0.2–0.3 mm) was placed inside a straight quartz column (o.d. 6 mm, 15 cm long). The column was installed in a standard gas chromatograph (Shimadzu 14A). Prior the measurements the zeolite was activated by prolonged heating (5 °C/min to 250 °C, ca 10 h) in a flow of He. After the activation the column temperature was adjusted and the IGC measurements were performed. Samples of the adsorbate (i.e. 10 μl of air saturated with the HC vapor) were injected manually using a gas-tight chromatographic syringe.

3. Results

The QE-TPDA profiles of *n*-hexane and *n*-heptane observed for zeolites X and Y are presented in Fig. 1. All profiles exhibit one desorption maximum and one corresponding adsorption minimum, that should be attributed to the molecules adsorbed in the supercages of the FAU structure. These results are in agreement with the previously reported findings [5,6,8,9]. Much higher desorption temperatures observed for zeolites X than for Y may results from the interactions of the adsorbed molecules with the extraframework Na^+ cations or the framework Al atoms. The latter effect may be also a reason of a slightly stronger adsorption of *n*-alkanes in Y(17).

The results obtained for ZSM-5 and beta (shown in Fig. 2) are different from those found for X and Y. Complex two-step adsorption and desorption profiles observed for the MFI type structure have been earlier attributed to the “commensurate freezing” effect, occurring at adsorption degree above 4 molecules per unit cell (50% of the maximum sorption capacity) [12]. Similar desorption patterns were reported also for other zeolites possessing three-dimensional system of intersecting micropores (5A [13], ZSM-11 [9]). A kind of two-step QE-TPDA profiles were observed also for zeolite beta. How-

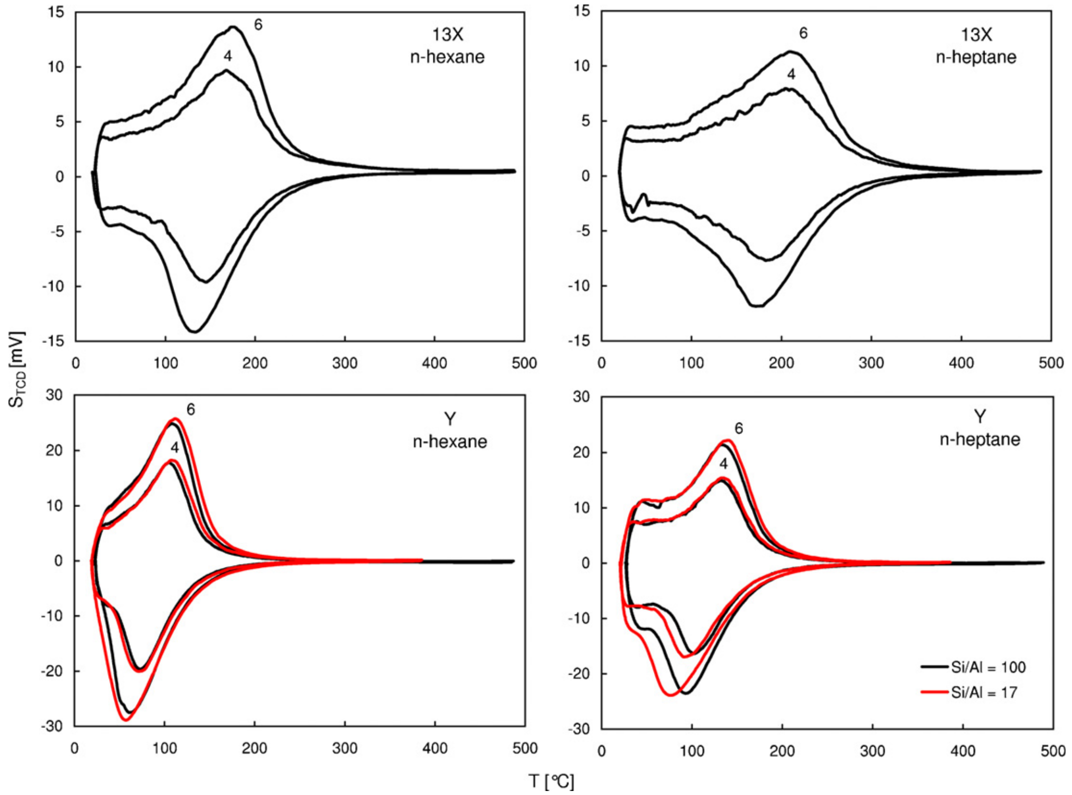

Fig. 1. The QE-TPDA profiles of *n*-hexane and *n*-heptane on zeolites 13X and Y, measured at 4 and 6° K min^{-1} (values of the heating/cooling rate are shown in the figure).

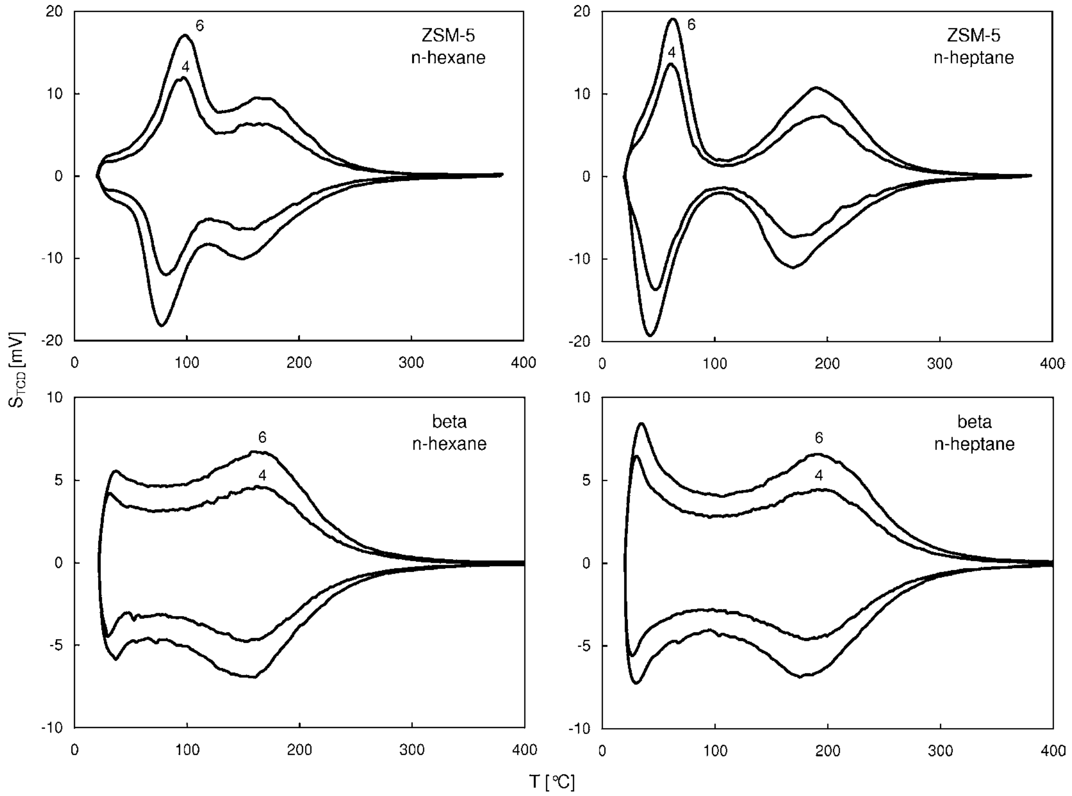

Fig. 2. The QE-TPDA profiles of *n*-hexane and *n*-heptane on zeolites ZSM-5 and beta, measured at 4 K min^{-1}.

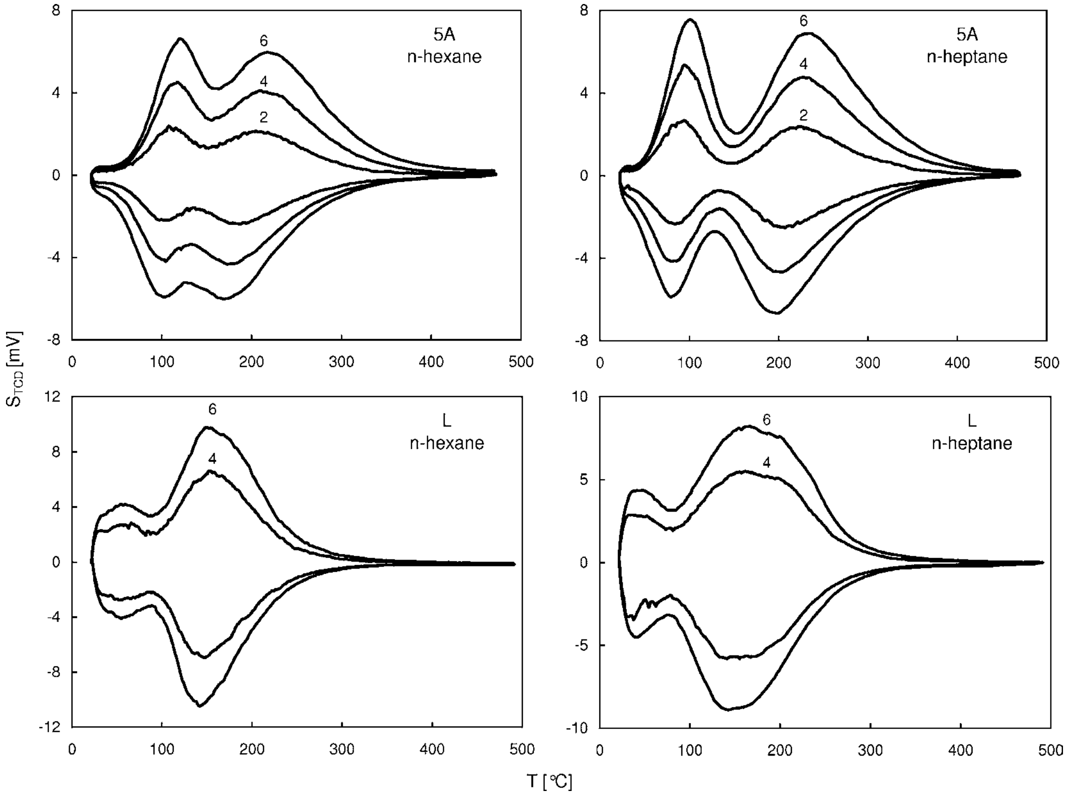

Fig. 3. The QE-TPDA profiles of *n*-hexane and *n*-heptane on zeolites 5A and L, measured at 2, 4 and/or 6° K min^{-1}.

ever, the high temperature (HT) adsorption/desorption peaks are much broader than those observed for ZSM-5, while the low temperature parts (LT) of the profiles hardly form complete peaks.

The QE-TPDA profiles observed for zeolites 5A and L (shown in Fig. 3) also reveal two-step adsorption patterns. Unlike for zeolite beta, their LT desorption maxima are located above the ambient temperature. The QE-TPDA profiles obtained for

Table 1
Parameters characterizing adsorption of *n*-hexane: maximum sorption capacity (a_{max}), pore volume (V_{por}), adsorption enthalpy and entropy, determined from the QE-TPDA profiles by fitting the Langmuir or Henry adsorption functions, and values of the initial adsorption heat determined using infinite dilution IGC

Sorbate	Zeolite	a_{max}	V_{por}	Langmuir/DSL fit		Henry fit		IGC
		(mmol g^{-1})	(cm^3 g^{-1})	$-\Delta H_{ads}$ (kJ mol^{-1})	$-\Delta S_{ads}$ (J mol^{-1}K^{-1})	$-\Delta H_{ads}$ (kJ mol^{-1})	$-\Delta S_{ads}$ (J mol^{-1} K^{-1})	$-\Delta H_{ads}$ (kJ mol^{-1})
Hexane	ZSM-5	1.12	0.165	67[a]	110[a]	59	99	68
				102[a]	236[a]			
	13X	1.67	0.246	62	95	47	69	51
	Y(17)	1.74	0.256	64	131	44	82	42
	Y(100)	1.57	0.231	65	135	44	82	40
	Beta	1.10	0.162	57	87	53	85	
	5A	1.22	0.160	59[a]	82[a]	61	90	
				79[a]	168[a]			
	L	1.25	0.164	58[a]	90[a]	56	88	
				53[a]	121[a]			
Heptane	ZSM-5	1.23	0.161	75[a]	117[a]	68	109	
				89[a]	224[a]			
	13X	1.84	0.240	65	89	54	73	60
	Y(17)	1.90	0.248	69	129	49	84	45
	Y(100)	1.72	0.224	69	129	48	83	44
	Beta	1.13	0.147	63	88	61	90	
	5A	1.18	0.173	65[a]	124[a]	52	103	
				74[a]	198[a]			
	L	1.19	0.175	42[a]	84[a]	58	122	
				56[a]	169[a]			

[a] Peak positions.

zeolites L, 5A and ZSM-5 exhibit similar shifts of the peak positions upon change from *n*-hexane to *n*-heptane – the HT peaks are shifted to higher temperatures, but the LT peaks – to lower ones, while for zeolite beta an inverse shift of the LT peak position is found. The relative share of the LT peaks decrease in the series ZSM-5 > 5A > L.

It may be noticed that for zeolite 5A the desorption and adsorption profiles are not quite equivalent. A delay of desorption at the high temperature limit and of adsorption at low temperatures observed for higher heating/cooling rates clearly results from diffusion limitations, most probably related to close matching of the kinetic diameter of *n*-alkane molecules to the free aperture of the micropores in CaNa-LTA framework. However, these limitations practically disappear when the temperature change rate as low as 2 K/min is used.

Values of the saturation adsorption capacity obtained by integration of the QE-TPDA profiles, are listed in Table 1, together with values of the micropore volume that were calculated from the adsorption capacities, assuming the density of the adsorbate equal to that of liquid. The sorption capacity values are close to the literature data and the micropore volumes are similar to those obtained from low temperature N_2 adsorption isotherms [9,15,16].

Although zeolites beta, Y and ZSM-5 were studied in the hydrogen-exchanged (acidic) forms, no undesired side effects due to catalytic cracking of *n*-alkanes or coking were observed, mainly because of both low concentration of the acid sites (i.e. high Si/Al ratio) and low partial pressure of the adsorptive. Such undesired effects were observed earlier only for QE-TPDA of *n*-nonane on much more acidic zeolites ZSM-5 (Si/Al = 15) and USY (framework Si/Al = 4.5) at temperatures above 300 °C [17]. The signal approaching zero at high temperature and very good reproducibility of the QE-TPED profiles obtained in cyclic experiments excluded any considerable cracking of *n*-alkanes or coking of the zeolites.

4. Discussion

Desorption and adsorption parts of the QE-TPDA profiles are similar, only positions of the adsorption minima are shifted to lower temperatures by ca 40° relative to the positions of the maxima. This shift is the smaller, the higher is the inlet concentration of the adsorptive and the smaller are the sample size or the heating/cooling rate. It may be expected that in the extreme case this shift will become negligible, provided that the equilibrium control of adsorption and desorption is maintained. In such a case a QE-TPDA profile should be regarded as a temperature derivative of the adsorption isobar, so that the isobar could be calculated by its integration.

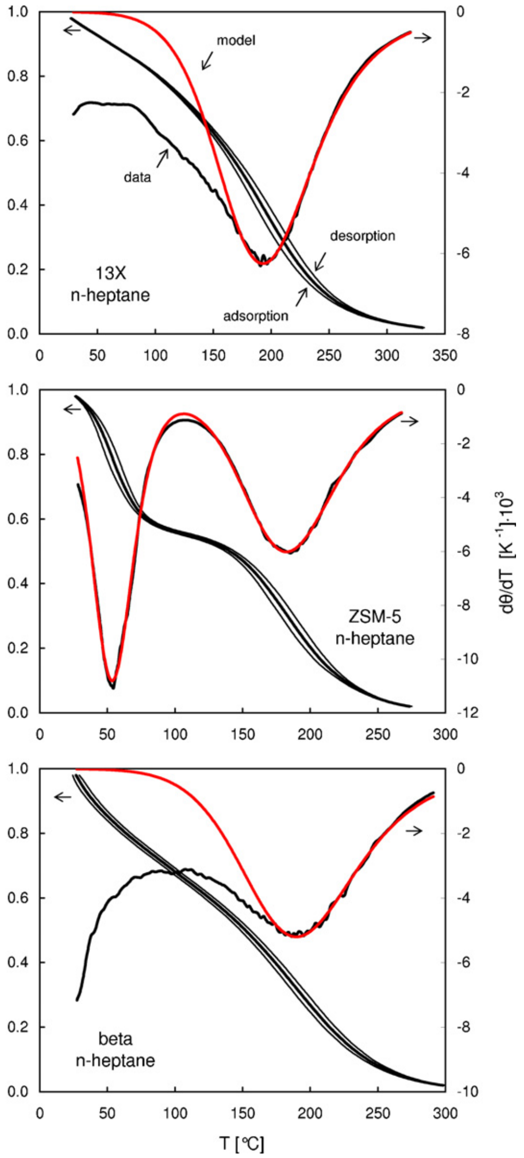

Fig. 4. The adsorption isobars (and their temperature derivatives) of *n*-heptane on zeolites 13X, ZSM-5 and beta determined from the QE-TPDA profiles measured at 4 K min^{-1} and p_{hept} = 3.0, 3.8 mbar or 4.2 mbar, respectively.

However, even when there is no perfect agreement between the desorption and adsorption profiles, the isobar could be approximated by averaging of the integrated QE-TPED profiles. Examples of such averaging for adsorption of *n*-heptane on zeolites 13X, ZSM-5 and beta are presented in Fig. 4. The adsorption and desorption profiles were integrated and the temperature dependence of the adsorption degree was calculated as

$$\theta(T) = 1 - \frac{A(T_0, T)}{A(T_0, T_f)} \tag{1}$$

where

$$A(T_0, T) = \int_{T_0}^{T} S_{\text{TCD}}\,\mathrm{d}t \tag{2}$$

The integrated desorption and adsorption profiles $\theta(T)$ were interpolated at chosen values of the adsorption degree (from 0.02 to 0.98, with 0.002 step). Then the approximate isobar was calculated by averaging temperatures corresponding given values of θ

$$T_\theta = \frac{(T_{\text{des}})_\theta + (T_{\text{ads}})_\theta}{2} \tag{3}$$

To the temperature derivatives of the averaged isobars, calculated by their numerical differentiation, the Langmuir model functions were fitted

$$\frac{\mathrm{d}\theta}{\mathrm{d}T} = \frac{\Delta H_{\mathrm{ads}}\, p \exp(-\Delta G_{\mathrm{ads}}/RT)}{[1 + p \exp(-\Delta G_{\mathrm{ads}}/RT)]^2 RT^2} \tag{4}$$

$$\Delta G_{\mathrm{ads}} = \Delta H_{\mathrm{ads}} - T\Delta S_{\mathrm{ads}} \tag{5}$$

where T is the temperature, p the relative partial pressure of the adsorptive ($p = p_i/p^{\circ}$), ΔH_{ads} and ΔS_{ads} are adsorption enthalpy and entropy (for the standard pressure p°).

For the 13X zeolite quite good agreement of fitting was observed in the high temperature range above 180 °C (cf. Fig. 3). Similar quality of fitting (not shown here) was obtained for the other *n*-alkane/FAU-type zeolite systems. The fact that the experimental data deviate from the model function at lower temperatures confirms that the Langmuir adsorption model, not taking into account the intermolecular interactions, is too simple for description of adsorption of *n*-alkanes in the FAU structure [7]. The values of the adsorption enthalpy and entropy ($-\Delta H_{\mathrm{ads}} = 65\,\mathrm{kJ\,mol^{-1}}$, $-\Delta S_{\mathrm{ads}} = 89\,\mathrm{J\,mol^{-1}\,K^{-1}}$), obtained as the fitted parameters, do not differ considerably from those calculated by fitting the quasi-equilibrium model to the QE-TPD data ($-\Delta H_{\mathrm{ads}} = 70\,\mathrm{kJ\,mol^{-1}}$, $-\Delta S_{\mathrm{ads}} = 97\,\mathrm{J\,mol^{-1}\,K^{-1}}$ [5]). This indicates that the method proposed here gives a good approximation of the adsorption isobars. However, an arbitrary choice of the low temperature limit for fitting the Langmuir model results in relatively high uncertainty of the adsorption parameters (exceeding 5 kJ mol^{-1} for the adsorption heat).

In the case of ZSM-5 zeolite, the differential isobars were fitted with the DSL function, i.e. the linear combination of two Langmuir model functions (Eq. (4)). Very good fit was observed in the whole temperature range (cf. Fig. 4). Values of the fitted parameters for *n*-heptane (HT peak: $-\Delta H_{\mathrm{ads2}} = 75\,\mathrm{kJ\,mol^{-1}}$, $-\Delta S_{\mathrm{ads2}} = 117\,\mathrm{J\,mol^{-1}\,K^{-1}}$ and LT peak: $-\Delta H_{\mathrm{ads1}} = 89\,\mathrm{kJ\,mol^{-1}}$, $-\Delta S_{\mathrm{ads1}} = 224\,\mathrm{J\,mol^{-1}\,K^{-1}}$) are close to those obtained earlier by fitting the quasi-equilibrium model ($-\Delta H_{\mathrm{ads2}} = 75\,\mathrm{kJ\,mol^{-1}}$, $-\Delta S_{\mathrm{ads2}} = 119\,\mathrm{J\,mol^{-1}\,K^{-1}}$ and $-\Delta H_{\mathrm{ads1}} = 96\,\mathrm{kJ\,mol^{-1}}$, $-\Delta S_{\mathrm{ads1}} = 245\,\mathrm{J\,mol^{-1}\,K^{-1}}$, respectively [5]). They are in agreement with the commensurate freezing concept, attributing the high temperature peak to adsorption in the micropores and the low temperature peak to ordering of the adsorbed molecules, accompanied by second adsorption step.

Although the averaged QE-TPDA profile of *n*-heptane for zeolite beta seems to consist of two desorption maxima, it could not be accurately fitted with the DSL function. Fitting the Langmuir function to the high temperature maximum gave reasonable value of $-\Delta H_{\mathrm{ads}} = 57\,\mathrm{kJ\,mol^{-1}}$, only slightly higher than 51 kJ mol^{-1} obtained by fitting the same model function to the adsorption isotherms data [14].

The adsorption isobars of *n*-heptane, determined by averaging of the integrated QE-TPDA profiles for zeolites 5A and L, along with their two peak temperature derivatives fitted with the DSL functions, are shown in Fig. 5. In the case of zeolite 5A very good fit was obtained for both *n*-hexane and heptane, and values of the adsorption enthalpy are in agreement with the literature data obtained by fitting the Langmuir function to the adsorption isotherms [18]. For zeolite L good fit was obtained for *n*-hexane, while for *n*-heptane the high temperature part of the differential isobar clearly deviates from the model function. The fact that for zeolite L the QE-TPDA profiles of *n*-hexane and *n*-heptane differ in shape, the latter being much broader, may be an evidence of sorbate–sorbate interactions or a transition in the adsorbed phase, more enhanced for larger molecules. This observation is supported by the values of the adsorption enthalpy and entropy that depend on both position and width of the thermodesorption peak, corresponding to the HT desorption step. Those obtained for *n*-hexane on zeolites L and beta (having almost the same diameter of the micropores) are very close and quite reasonable, while much lower values of ($-\Delta H_{\mathrm{ads2}}$) and ($-\Delta S_{\mathrm{ads2}}$) determined for *n*-heptane on zeolite L are by far underestimated.

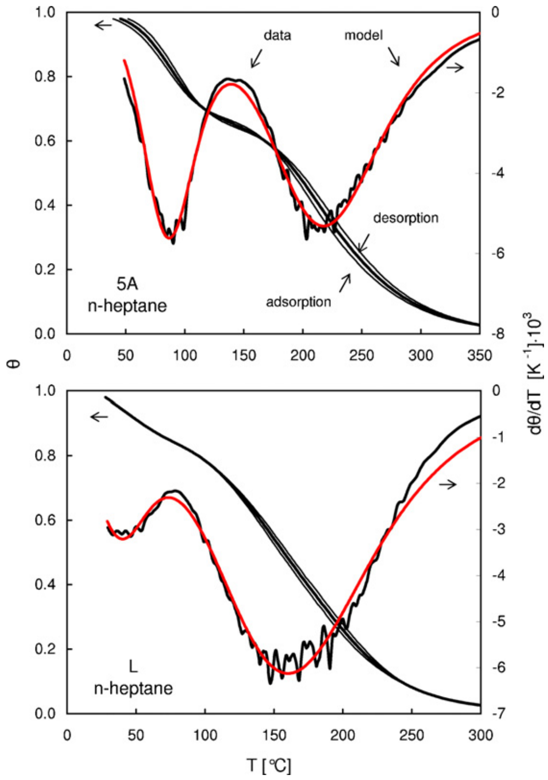

Fig. 5. The adsorption isobars (and their temperature derivatives) of *n*-heptane on zeolites 5A and L, determined from the QE-TPDA profiles measured at 2 or 4° K min^{-1}and $p_{\mathrm{hept}} = 4.3$ or 5.5 mbar, respectively.

Model functions derived from the Langmuir model are frequently used for quantifying adsorption of *n*-alkanes on zeolites and determination of the adsorption heat [8,19,20]. However, despite quite good agreement with the experimental data, their use is often criticized, since the Langmuir model is too simple and does not encompass heterogeneity of the adsorption sites or sorbate–sorbate interactions. Therefore other methods of determination of the adsorption heat from the thermodesorption data should also be used. As it has been shown earlier [6], it is possible to obtain dependence of the adsorption enthalpy and entropy on the adsorption degree, basing on the isosters constructed from the set of the QE-TPDA data. However, in order to obtain accurate values of the isosteric adsorption enthalpy and entropy this approach requires high quality experimental data, free from diffusion limitations or major disturbances of the detector signal even for a quite high heating/cooling rate.

We propose here another, much simpler method of calculation of the adsorption heat from the QE-TPDA profiles, limited to the initial (zero-coverage) range of adsorption. It is based on the Henry adsorption function which may be regarded as the simplified Langmuir function, obtained by assuming the term pK_{ads} negligible when compared to 1:

$$\theta = K_{\mathrm{ads}}p = p\exp\left(-\frac{\Delta G_{\mathrm{ads}}}{RT}\right) \tag{6}$$

High temperature range of the differential experimental isobar may be fitted with the temperature derivative of the Henry function

$$\frac{\mathrm{d}\theta}{\mathrm{d}T} = \frac{\Delta H_{\mathrm{ads}}p}{RT^2}\exp\left(-\frac{\Delta G_{\mathrm{ads}}}{RT}\right) \tag{7}$$

It may be transformed to a linear function of $1/T$

$$\ln\left(-\frac{\mathrm{d}\theta}{\mathrm{d}T}T^2\right) = \ln\left(-\frac{\Delta H_{\mathrm{ads}}p}{R}\right) + \frac{\Delta S_{\mathrm{ads}}}{R} - \frac{\Delta H_{\mathrm{ads}}}{RT} \tag{8}$$

enabling easy determination of ΔH_{ads} and ΔS_{ads} by linear regression.

Examples of fitting the linearized Henry function to the transformed derivatives of the experimental isobars of *n*-heptane are presented in Fig. 6 (for zeolites 13 X, ZSM-5 and beta) and in Fig. 7 (for 5A and L). In all cases the high temperature parts of the transformed isobars show very good linearity. Moreover, the transformed isobars computed from the QE-TPDA profiles generally do not depend on the heating/cooling rate, thus confirming the equilibrium control of thermodesorption. The only exception to this rule is zeolite 5A exhibiting slightly lower slope of the transformed HT isobar for heating/cooling rates higher than 2 K min^{-1} due to diffusion limitations.

Values of the initial adsorption enthalpy determined from the QE-TPDA data were verified by means of the inverse gas chromatography (IGC) infinite dilution technique. This technique is based on measurements of chromatograms of small pulses of pure adsorbate through a column packed with the studied adsorbent. The concept of infinite dilution refers to very small partial pressures of the adsorptive, corresponding to the Henry range of the adsorption isotherm [4]. For this range the chromatograms are symmetrical and their retention times do not depend on the pulse size. The retention volume V_{g}, calculated from the retention time as

$$V_{\mathrm{g}} = (t_{\mathrm{R}} - t_{\mathrm{M}})F_{\mathrm{a}}\frac{T}{T_{\mathrm{a}}}j \tag{9}$$

$$j = \frac{2}{3}\left[\frac{(p_i/p_0)^2 - 1}{(p_i/p_0)^3 - 1}\right] \tag{10}$$

where t_{R} is the total retention time, t_{M} the retention time of non-adsorbing gas (air), T the column temperature, T_{a} the ambient temperature and j is the James-Martin compressibility factor, p denotes the carrier gas pressure: p_0 at the column outlet, p_i at the column inlet), is proportional to the Henry adsorption equilibrium constant [3,4]. Hence, the adsorption enthalpy may be calculated from its temperature dependence:

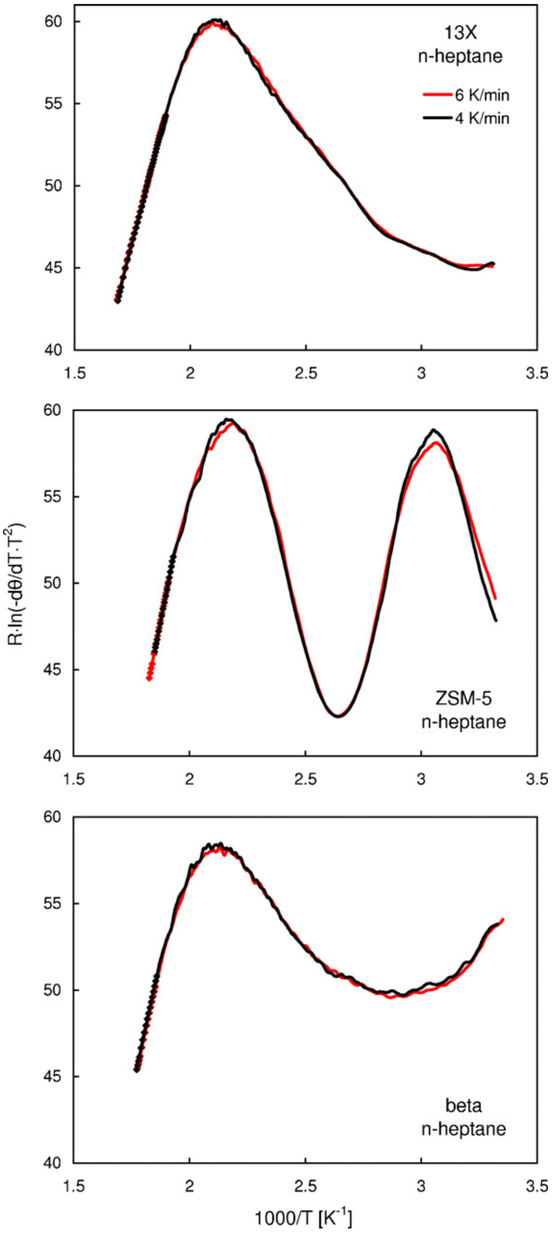

Fig. 6. Transformed differential adsorption isobars of *n*-heptane on zeolites 13X, ZSM-5 and beta determined from the QE-TPDA profiles measured at 4 and 6° K min^{-1}. The straight lines represent the linearized Henry adsorption function fitted to the high temperature data.

$$\Delta H_{\mathrm{ads}} = -R\left(\frac{\partial \ln V_{\mathrm{g}}}{\partial(1/T)}\right) \tag{11}$$

The corresponding plots of $\ln V_{\mathrm{g}}$ versus $1/T$, obtained from the IGC data for both studied alkanes on zeolites X, Y and ZSM-5 are shown in Fig. 8A. Values of the initial adsorption heat determined from the slopes of these plots are listed in Table 1. They are quite close to the corresponding values obtained from the QE-TPDA results: for ZSM-5 zeolites

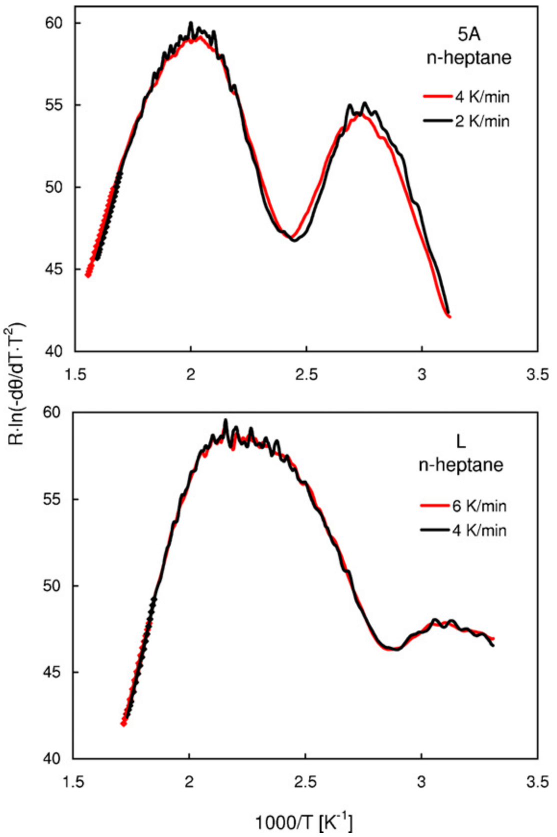

Fig. 7. Transformed differential adsorption isobars of *n*-heptane on zeolites 5A and L determined from the QE-TPDA profiles measured at 2, 4 and/or 6 K min^{-1}, with the linearized Henry function fitted to the high temperature data.

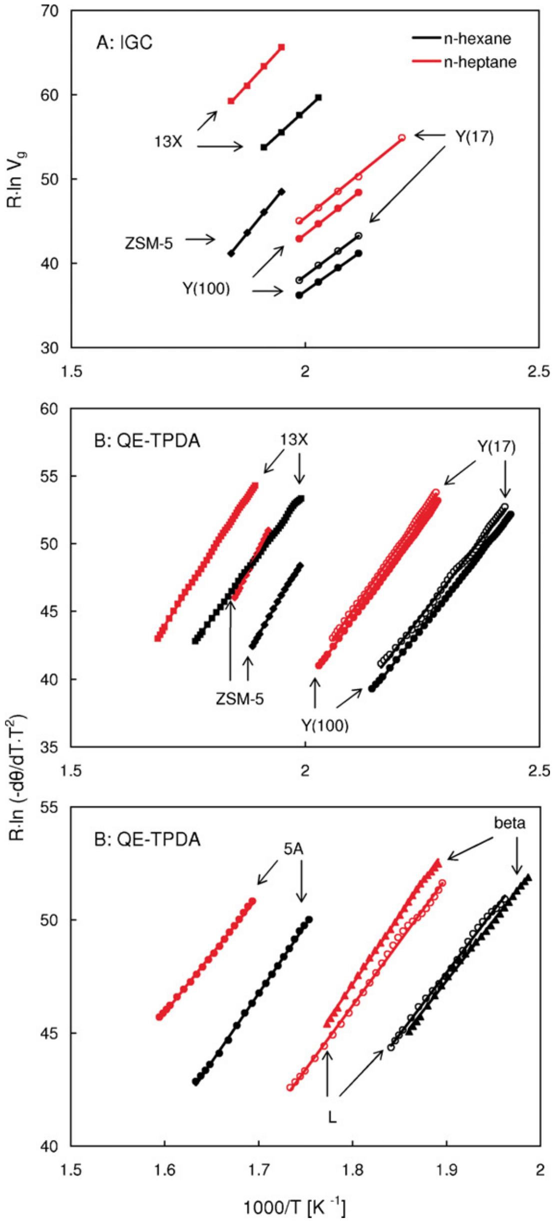

Fig. 8. Fitting the Henry-type adsorption functions to the IGC (A) and QE-TPDA (B) data for all the studied zeolites. Values of the adsorption heat determined as the fitted parameters are listed in Tables 1 and 2.

the IGC values are slightly higher, while for FAU-type zeolites they are lower by only 2–6 kJ mol^{-1} than the QE-TPDA values.

Results of fitting the linearized Henry function to high temperature parts of the transformed experimental data for both adsorbates and all the studied zeolites are shown in Fig. 8B. Values of adsorption enthalpy and entropy found as the fitted parameters are listed in Table 1, together with those obtained by fitting the Langmuir or DSL functions. As ΔH_{ads} and ΔS_{ads} values determined for different heating/cooling rate β were similar, only those found for the lowest heating/cooling rate used are shown.

Values of the initial adsorption heat determined from the QE-TPDA and IGC data shown in Table 1 may be compared with the available literature data listed in Table 2. The experimental values lower by 2–10 kJ mol^{-1} than the literature values indicate relatively low accuracy of the QE-TPDA method. Systematic underestimation of the initial adsorption heat may result not only from experimental errors due to imperfect instrumentation and experimental procedures but also form diffusion limitations. The latter source of uncertainty seems more important for *n*-heptane, as the corresponding differences between the experimental and the literature values are larger. The IGC values are also slightly underestimated, most probably because of not strict complying with the infinite dilution model. However, it should be pointed out that both the QE-TPDA and IGC values of the initial adsorption heat reproduce all differences between the studied zeolites, reported in the literature.

The adsorption enthalpy and entropy values ($-\Delta H_{\mathrm{ads}}$ and $-\Delta S_{\mathrm{ads}}$) determined using the Henry adsorption function are quite close to those obtained by fitting the Langmuir function. Major differences of these parameters, observed for X and Y zeolites may attributed to heterogeneity of the adsorption sites, related to different curvature of the micropores. For FAU-type framework, comprised of large supercages (1.3 nm in diameter) interconnected by 12 member-ring windows (0.7 nm) such heterogeneity is more likely than for MFI and BEA structures, in which the intersections are only slightly larger than the channels. Differences in the adsorption enthalpy and entropy values determined using both models for zeolite L, observed only in

Table 2
The literature values of the initial adsorption heat, determined from the adsorption measurements or molecular simulations

Sorbate	Zeolite	$-\Delta H^{\text{ads}}$ (kJ mol^{-1})
Hexane	ZSM-5	68.8[a], 66.0[b], 71.2[c]
	Y	45.5[a], 46.8[d]
	13X	54.1[e], 55.1[d]
	Beta	62.7[a], 63.4[f]
	5A	59.4[g], 60.8[h]
Heptane	ZSM-5	79.6[a], 86[b], 81.5[c]
	Y	51.9[a], 53.0[d]
	13X	61.6[e], 62.9[d]
	Beta	72.6[a]
	5A	69.4[h], 71.6[i]

[a] IGC, ZSM-5 (Si/Al = 137), NaY (Si/Al = 2.7) and beta (Si/Al = 12) [21].
[b] IGC, for silicalite-1 (Si/Al = 400) [22].
[c] Molecular simulations, silicalite-I, calculated according to [23].
[d] Molecular simulations, NaY (Si/Al = 2.76) and NaX (Si/Al = 1.28) [24].
[e] Gravimetry, NaX (Si/Al = 1.28) [25].
[f] ZLC, (Si/Al = 150) [14].
[g] Gravimetry [26].
[h] Molecular simulations, NaY (Si/Al = 2.76) and NaX (Si/Al = 1.28) [27].
[i] From adsorption isotherms (references in [27]).

the case of *n*-heptane may not be easily explained. Lowering of the ($-\Delta H_{\text{ads2}}$) and ($-\Delta S_{\text{ads2}}$) values found by fitting the DSL function results from broadening of the HT desorption peak, but the origin of this effect in not clear.

The values of ($-\Delta H_{\text{ads}}$) and ($-\Delta S_{\text{ads}}$) seem to increase with decreasing diameter of the micropores in a series FAU > (BEA, LTL) > (MFI, LTA). However, the values found for zeolite 5A (with LTA structure comprising micropores formed by 8 MR windows) are clearly lower that those obtained for ZSM-5 (with MFI structure comprising 10 MR channels). Differences observed for FAU-type zeolites should be explained by the presence of Na^+ cations in the micropores of 13X, resulting in a decrease of the effective micropore diameter. Higher adsorption heat observed for Y(17) zeolite with higher Al content may be attributed to interactions of the adsorbed molecules with the Bronsted acid sites [7] or with the framework Al atoms.

Although for microporous solids such as zeolites Langmuir-shaped type I adsorption isotherms should be expected, for most of the studied zeolites two-step adsorption patterns were observed. Such behavior was extensively studied for ZSM-5 zeolites [8,10,11,12,19] and reported for 5A [13], but for zeolites beta and L simple one-step adsorption profiles were observed [14,15]. Large values of the adsorption entropy ($-\Delta S_{\text{ads1}}$) found for the LT desorption peak by fitting the DSL functions indicate high degree of ordering of the adsorbed molecules in zeolites 5A and L. Such ordering may be attributed to 3D system of interconnected micropores in LTA structure or to periodic changes in diameter of parallel channels in LTL structure, forming 1D system of micropores.

Despite apparent similarity between their frameworks, the zeolites ZSM-5 and beta exhibit significant differences in their QE-TPDA profiles of *n*-hexane and *n*-heptane, indicating differences in the interactions of the adsorbed molecules with the zeolite framework, especially for high adsorption degrees. The peaks observed for the zeolite beta are broader (which is reflected by smaller values of $-\Delta H_{\text{ads}}$ and $-\Delta S_{\text{ads}}$), moreover the low temperature peak is shifted to left in the case of n-heptane, while the opposite shift was found for ZSM-5. Unfortunately, the low temperature peaks for the zeolite beta could be only partially observed in the measurements starting at room temperature. Therefore for a complete characterization of adsorption of *n*-alkanes on zeolites beta further studies, covering also subambient temperature range, are necessary.

5. Conclusions

The results obtained indicate that adsorption of *n*-hexane and *n*-heptane on studied zeolites cannot be quantified using Langmuir adsorption model in the whole range of adsorption degree. Aproximate Langmuirian behavior may be expected only for high temperature adsorption range, for adsorption degrees below about 50% of the saturation sorption capacity. Complex QE-TPDA profiles observed clearly show that apart from the adsorption in the micropores in high temperatures, other phenomena as sorbate–sorbate interactions or order–disorder transitions in the adsorbed phase affect the adsorption profiles in low temperatures.

It has been shown that the QE-TPED measurements may be used for determination of the approximated adsorption isobars. Values of the adsorption enthalpy and entropy may be computed by fitting the temperature derivatives of such isobars with the functions based on the Langmuir or Henry adsorption model. The values of initial (zero-coverage) thermodesorption adsorption parameters are equivalent to those obtained by means of the IGC infinite dilution method. Such values are thermodynamically correct, since the formalism of their computation is based on the Henry adsorption function, which is a limit case for majority of adsorption isotherms. Application of the QE-TPDA method for determination of the initial adsorption heat seems an interesting alternative to IGC and other experimental methods, especially in the case of strongly adsorbing microporous solids, such as zeolites.

The QE-TPED profiles of *n*-hexane and *n*-heptane observed for the zeolites 5A, X, Y and ZSM-5 are in agreement with the earlier results, while those found for beta and L reveal two-step adsorption patterns. The two-step QE-TPED profiles observed for zeolites L, 5A and ZSM-5 were accurately fitted with the DSL adsorption functions. Values of the adsorption enthalpy and entropy obtained as a fitted parameter indicate that also in the case of zeolites L and 5A ordering of the molecules adsorbed in the micropores may occur.

Acknowledgement

This work has been supported by the Ministry of Science and Higher Education of Poland with a grant number N507 108 32/3175.

References

[1] S. Sircar, D.V. Cao, Chem. Eng. Technol. 25 (2002) 10.
[2] H. Stach, K. Fiedler, J. Jänchen, Pure Appl. Chem. 65 (1993) 2193.

[3] F. Thielmann, J. Chromatogr. A 1037 (2004) 115.

[4] E. Díaz, S. Ordóñez, A. Vega, J. Coca, J. Chromatogr. A 1049 (2004) 139.

[5] W. Makowski, D. Majda, J. Porous Mater. 14 (2007) 27.

[6] W. Makowski, Thermochim. Acta 454 (2007) 26.

[7] F. Eder, J.A. Lercher, Zeolites 18 (1997) 75.

[8] B. Millot, A. Methivier, H. Jobic, J. Phys. Chem. 102 (1998) 3210.

[9] W. Makowski, D. Majda, Thermochim. Acta 412 (2004) 131.

[10] W. Makowski, D. Majda, Appl. Surf. Sci. 252 (2005) 707.

[11] V. Dondur, V. Rakić, L. Damjanović, R. Hercigonja, A. Auroux, J. Therm. Anal. Calorim. 84 (2006) 233.

[12] N.B. Smit, T.L.M. Maesen, Nature 374 (1995) 42.

[13] N. Sivasankar, S. Vasudevan, J. Phys. Chem. B 109 (2005) 15417.

[14] P.S. Bárcia, J.A.C. Silva, A.E. Rodrigues, Micropor. Mesopor. Mater. 79 (2005) 145.

[15] P.N. Joshi, U.D. Joshi, T.H. Kim, K.I. Kim, V.P. Shiralkar, Adsorption 7 (2001) 279–289.

[16] B. Röhl-Kuhn, P. Klobes, K. Meyer, P. Lorenz, B.M. Gawlik, A. Lamberty, H. Muntau, EUR Report 21065, Luxemburg, 2004, ISBN 92-894-7111-5.

[17] W. Makowski, P. Kuśtrowski, Micropor. Mesopor. Mater. 102 (2007) 283–289.

[18] J.A.C. Silva, A.E. Rodrigues, Ind. Eng. Chem. Res. 38 (1999) 2434.

[19] W. Zhu, F. Kapteijn, B. van der Linden, J.A. Moulijn, Phys. Chem. Chem. Phys. 3 (2001) 1755.

[20] E.N. Gribov, G. Sastre, A. Corma, J. Phys. Chem. B 109 (2005) 23794.

[21] J.F. Denayer, W. Souverijns, P.A. Jacobs, J.A. Martens, G.V. Baron, J. Phys. Chem. B 102 (1998) 4588.

[22] .C. Arik, J.F. Denayer, G.V. Baron, Micropor. Mesopor. Mater. 60 (2003) 111.

[23] E. García-Pérez, I.M. Torrens, S. Lago, R. Krishna, B. Smit, S. Calero, Stud. Surf. Sci. Catal. 158 (2005) 1097–1104.

[24] S. Calero, D. Dubbeldam, R. Krishna, B. Smit, T.J.H. Vlugt, J.F.M. Denayer, J.A. Martens, T.L.M. Maesen, J. Am. Chem. Soc. 126 (2004) 11376.

[25] M. Tarek, R. Kahn, E.C. de Lara, Zeolites 15 (1995) 67.

[26] M.J.A.C. Silva, A.E. Rodrigues, AIChE J. 43 (1997) 2524.

[27] E. García-Pérez, D. Dubbeldam, T.L.M. Maesen, S. Calero, J. Phys. Chem. B 110 (2006) 23968.